Three-dimensional analysis of patterns of skin displacement over the equine radius

D. H. SHA*, D. R. MULLINEAUX and **H. M. CLAYTON**

McPhail Equine Performance Center, College of Veterinary Medicine, Michigan State University, East Lansing, Michigan 48824, USA.

Keywords: horse; skin displacement; Fourier series; modelling; locomotion

Summary

***Reasons for performing study*: Surface markers are usually used to track bone movement. However, skin movement related to the bone has a large effect on the analysis of skeletal kinematics. A 2-dimensional (2D) skin displacement correction model has been successfully developed, but no 3D skin displacement model exists.**

***Objectives*: To develop a 3-dimensional (3D) skin displacement model for the equine radial segment during trot.**

***Methods*: The 3D trajectories of 6 skin-based markers and a bone-fixed triad were captured at trot in 4 horses. Skin displacements in the bone-based coordinate system were calculated using a singular-value decomposition method. The truncated Fourier series models were developed for the skin displacements using a generalised cross-validatory spline.**

***Results*: Mean ± s.d. of peak skin displacement of the 3 markers on the proximal radius as percentage of radial length was 10.7 ± 0.5, 4.6 ± 1.5 and 14.5 ± 2.9% in x, y and z direction, respectively. For the 3 markers on the distal radius, the equivalent displacements were 4.7 ± 0.6, 1.7 ± 0.8 and 7.3 ± 1.8% in x, y and z direction, respectively.**

***Conclusions*: The 3D skin displacement model for correction of skin marker motion over the equine radius relative to the bone can be established using a truncated Fourier series, which has previously been used successfully to develop 2D models.**

***Potential relevance*: This method of determining 3D skin displacement correction needs to be extended to the entire fore- and hindlimbs to provide a more sensitive measure of kinematic analysis. Accurate descriptions of the 3D motions of the limb segments and interactions between adjacent segments at the joints are necessary for understanding of the mechanics of different gaits and the gait aberrations that manifest as lameness.**

Introduction

Surface markers, usually used to track bone movement, have many advantages compared with invasive bone-fixed markers. However, skin movement related to the underlying bone has a large effect on the analysis of skeletal kinematics (Reinschmidt *et al.* 1997b). A 2-dimensional (2D) skin displacement correction model has been used successfully for kinematic analysis of the horse (van Weeren and Barneveld 1986; van Weeren *et al.* 1988; 1990a,b, 1992; van den Bogert *et al.* 1990), but no 3-dimensional (3D) skin displacement model exists.

Kinematics are especially sensitive to skin motion artefacts when skin surface markers are used to track segmental motion. Skin displacements relative to the underlying bone at some sites over the equine radius have a range of motion of up to 45 mm during a stride at trot (van Weeren *et al.* 1990b). Marker cluster design and placement can reduce some errors of kinematics of segments (Cappozzo *et al.* 1997). For example, a cluster made up 4 markers is a good choice. Planar clusters are acceptable if they are in quasi-isotropic distribution and the root mean square distance of the markers from their centroid should be >10 times the s.d. of the marker position error. The cluster should be placed on sites where there is minimal skin movement and on the lateral aspect of limbs to facilitate visualisation for recording purposes and to avoid interference during motion. The actual underlying bone motion is still difficult to reproduce, however, even when utilising a redundant marker set and a least-squares estimator of the transformation data to calculate kinematics (Reinschmidt *et al.* 1997b).

Kinematic data recorded from bone-fixed markers have been used to calculate the true *in vivo* kinematics of joints in human subjects (Reinschmidt *et al.* 1997a) and in horses (van Weeren *et al.* 1992; Lanovaz *et al.* 2002). The use of bone-fixed markers is invasive and it is desirable to develop procedures that avoid surgical intervention but still produce an acceptable degree of accuracy.

Skin displacement artefact correction models have been shown to improve joint angular data over noncorrected 2D kinematics (van den Bogert *et al.* 1990; van Weeren *et al.* 1992). In developing a model, methods available include linear regression and nonlinear regression, such as polynomials. For a data set with a simple pattern and correlation with some variables, linear regression is best (van Weeren *et al.* 1988) but for a periodic data set with a complicated pattern and without any correlation with other variables, a Fourier series may be the best and most intuitive method (Cappozzo *et al.* 1975). The present studies build upon the methodologies cited above to develop 3D skin correction algorithms at the trot.

The first step in developing a skin displacement artefact correction model is to characterise the 3D motion of the skin relative to the bone. The radial segment was selected to illustrate the skin displacement procedure for 2 reasons; first, skin displacements appear to be small for the metacarpus compared

*Author to whom correspondence should be addressed.
[Paper received for publication 10.05.04; Accepted 08.10.04]

TABLE 1: Marker locations at the radius in the standing pose from the origin of the radial bone coordinate system (BCS) (the midway point between Rad-6 and C). Data are means ± s.d. expressed as % of segment length in local BCS (x, y, and z represent cranial/caudal, medial/lateral and proximal/distal directions, respectively)

Marker	x	y	z
Rad-1	0 ± 3	-29 ± 4	98 ± 0
Rad-2	-12 ± 3	-20 ± 3	63 ± 2
Rad-3	19 ± 2	-27 ± 6	80 ± 1
Rad-4	9 ± 7	-10 ± 4	28 ± 16
Rad-5	-14 ± 1	-11 ± 2	24 ± 8
Rad-6	-1 ± 0	-15 ± 0	0 ± 0

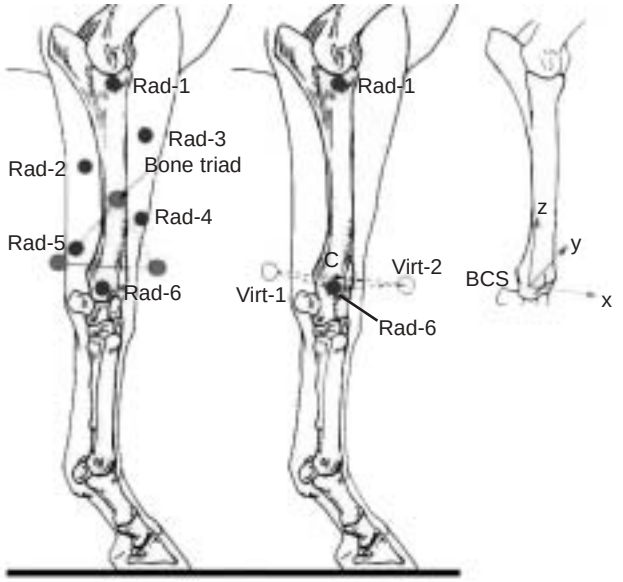

Fig 1: Six skin-based marker positions (Rad-1–6, ●) on the radius of right forelimb used to calculate skin displacements. Three bone-fixed markers (●) were used for calculating the true kinematics of bone movement. Two additional markers (Virt-1 and Virt-2, ○) on the medial side of the limb (midway point C) were used to calculate the local bone coordinate system as illustrated (x = cranial/caudal, y = medial/lateral and z = proximal/distal directions). These 2 virtual markers were at the same level as skin marker Rad-6 and were removed during data collection.

with the radius (van Weeren *et al.* 1990b), and second, the large muscle mass on the lateral aspect of the limb makes it difficult to insert pins in the more proximal segments. Therefore, the radial segment offers a site on the lateral aspect of the limb that is easily accessible for percutaneous insertion of a bone pin. Three-dimensional analysis requires a minimum of 3 markers per segment, but optimal marker placement sites are not known. The aim of the study was to collect simultaneous kinematic data from skin surface and bone-fixed markers from the radius of equine subjects to parameterise the general motion of skin marker sites relative to the underlying bone, to determine which marker sites show least displacement, and to use these parameters to develop a model of the skin motion and a correction procedure.

Materials and methods

Subjects

With approval of the Institute's Committee on Animal Use and Care, 4 sound horses were used. The physical data for the subjects were mean ± s.d. mass 433 ± 63 kg, length of radius 0.369 ± 0.013 m and height 1.47 ± 0.06 m.

Bone-fixed markers

A detailed explanation of the procedure for fixing markers to bone has been presented elsewhere (Lanovaz *et al.* 2002). In summary, 4.75 mm diameter Steinmann pins were inserted percutaneously under general anesthesia into the radius of the right forelimb of the subjects. The insertion site was on the craniolateral side of the bone, proximal to the lateral styloid process, where the bone is placed subcutaneously. A marker triad consisting of three 25 mm diameter reflective spherical markers was attached rigidly to the pin during the data collection session. Analgesics were administered systemically and locally, and all subjects appeared pain-free and moved willingly and normally during data collection, which took place approximately 24 h after surgery.

Skin-based markers

In addition to the bone-fixed marker triad, a set of six, 25 mm diameter spherical reflective markers, Rad-1 to Rad-6, were attached at predetermined locations on the surface of the skin over the right radius of each subject (Fig 1). The skin markers were located as triads representing the proximal and distal ends of the bone. Marker locations from the standing poses are showed in Table 1. The distance between markers Rad-1, overlying the radial tuberosity, and Rad-6, overlying the lateral styloid process, served as the reference length for the radius. The skin-based markers were distributed over the lateral aspect of the segment, since most studies track kinematic data from the lateral side. Placement of the radial markers was such that it minimised merging with the bone pin marker triads both in the standing position and during locomotion.

Bone coordinate systems

To define a local bone-based coordinate system (BCS), all subjects were placed in a normal standing position and 2 additional markers were used to locate the medial styloid process. These markers, Virt-1 and Virt-2, were attached to a rod, the centre of which was placed over the medial styloid process. These virtual markers protruded on the cranial and caudal sides of the limb when it was viewed from the lateral side, with the medial styloid process midway between them (Fig 1b). They were removed before collecting data at the trot.

The motion analysis system tracks the marker locations within a global coordinate system (GCS). For 3D analysis of limb kinematics, the marker locations are transposed into a bone-based coordinate system that expresses segmental motion in an anatomically meaningful manner. A right-handed coordinate system was developed for the radius by first defining the flexion/extension axis (y) as the vector running from Rad-6 to the medial styloid process which was the middle point (C) between the 2 virtual markers (Virt-1 and Virt-2). The adduction/abduction axis (x) of the radius was defined as a vector pointing cranially and perpendicular to the plane formed by the flexion/extension axis (y) and the vector running from Rad-6 to Rad-1. Finally, the internal/external rotation axis (z) of the radius was defined as a vector pointing proximally from Rad-6 to Rad-1 along the long axis of the bone and

perpendicular to the plane formed by the flexion/extension and adduction/abduction axes. The origin of the radius BCS was embedded in the bone midway between Rad-6 and C.

Data collection and preprocessing

All subjects were led in hand at the trot along a 40 m rubber-covered concrete runway. Three-dimensional kinematic data were collected using a 6 videocamera analysis system with software (RealTime3.2)[1] recording at 120 Hz. A volume measuring 5 x 2 x 3 m was calibrated and the mean error in measuring a known length within the volume was 0.88 mm. Each successful trial consisted of a single stride of the right forelimb, starting with stance. Data collected from a force platform (LG-6-4-8000)[2] embedded in the runway was used to detect the onset and termination of the right forelimb stance. The kinematic data from the trot trials were filtered using a fourth-order Butterworth filter with a cut-off frequency of 12 Hz. The length of data was normalised as 101 points for a full stride. The bone-fixed triad and skin-based markers were tracked simultaneously for each trial. At least 5 trials from each horse were selected. Trials were selected to match closely the forward velocities between subjects in the range 3–3.3 m/secs.

Reference kinematics

The 3D kinematics of the radius, as calculated by the motion of the bone-fixed triads was defined as the 'true' reference kinematics of the bone. The orientation matrices and displacement vectors for the reference kinematics were calculated by relating the locations of the triad of markers in the BCS of the radial segment with their GCS locations during each frame of motion data using a singular value decomposition method (SVD; Soderkvist and Wedin 1993).

Skin displacement and modelling

The 3D movements of the skin-based markers in the GCS were collected for the motion data. The data from each frame were transformed using the orientation matrices $R(t)$ and displacement vectors $a(t)$ calculated from the bone-fixed triads and expressed in terms of their corresponding BCS. So the skin displacements were calculated by

$$D(t) = [R(t)p_s^0 + d(t) - p_s(t)]/L$$

where $p_s(t)$ is the position of each skin-based marker in the GCS at time t during movement, p_s^0 is the position of each skin-based marker in the BCS at standing pose, L is the length of segment. The data from each subject were normalised to a percentage reference length of the radial segment calculated from the standing pose. The mean skin displacements of the group for each coordinate of each marker (Rad-1 to Rad-6) were calculated by $D(t) = \frac{1}{n}\Sigma_{i=1}^{n} D_i(t)$, $n = 4$ (4 subjects) except for Rad-3 ($n = 3$) and were parameterised by representing the data as an nth-order truncated Fourier series model (Cappozzo *et al.* 1975; van Weeren *et al.* 1992) given by

$$\hat{D}_n(t) = p_0 + \sum_{k=1}^{n} p_k \cos\left(\frac{2\pi kt}{100}\right) + \sum_{k=1}^{n} q_k \sin\left(\frac{2\pi kt}{100}\right)$$

where $\hat{D}_n(t)$ is an x, y or z coordinate of a skin-based marker, t is time as a percentage of stride, p_0 is a mean offset from the standing pose, p_k and q_k are Fourier series parameters and n is the number of harmonics used to describe the data.

To determine n for each coordinate, the mean values of all subjects were fit to Equation 1 using a standard linear least-squares method. A generalised cross-validation (GCV) criterion method (Woltring 1986, 1990) was used to find the statistically optimal n for each coordinate of each marker and the Fourier parameters p_0, p_k and q_k were then calculated. The optimal harmonic order n_{opt} was obtained by minimising the criterion function:

$$n_{opt} = \frac{RMS_n}{\mathrm{u}(N - 2n - 1)}$$

where $RMS_n = \frac{1}{N}\,\mathrm{u}(\Sigma_{t=1}^{N}[\bar{D}(t) - \hat{D}_n(t)])$

(root mean square) is fitting residual error, N is the length of the dataset (i.e. 101) and n is index of order of harmonics from the minimal value 1 to the maximal value 10.

As an estimate of the goodness of fit for all subjects, the RMS fit error between the model and the actual group data was calculated for each coordinate of each marker. The RMS and peak-to-peak amplitudes of the skin displacement for each coordinate of each marker were calculated from the fitted Fourier parameters.

Results

The mean ± s.d. stride duration was 706 ± 16 msecs, and stance percentage was 43.5 ± 2.4% of total stride duration. The reconstructions of skin displacements from the truncated Fourier series model indicated a good fit between the model and the skin displacement of the 4 horses, as shown by the fact that the pattern of the s.d. follows that of the fitted skin displacement curve (Fig 2). It is difficult to distinguish the curves representing the model and the mean of actual measurements. The skin displacements based on all subjects' mean values and the standard deviations between subjects are given on the same graph to enable visualisation of any variation between horses. The mean values for the standing pose locations of the markers relative to the radial BCS are given in Table 1. Variability in placement of markers Rad-1 and Rad-6 is low, due to the fact that these markers were placed over easily palpable bony landmarks. The values for the Fourier model parameters for the radial markers are given in Table 2. The data are presented as a percentage of segment reference length.

The optimal number of harmonics (n_{opt}), mean offset from the standing pose location (p_0), fitting error between the model and actual skin displacement (RMS), and peak-to-peak amplitudes of the skin displacement models along with maximal standard deviations between subjects (Max s.d.) are summarised in Table 3. The peak-to-peak amplitude of skin displacement for the radial markers ranged from 0.8 to 17.8% of the segment length, with the average being 7.2% of segment length. This corresponds to an approximate displacement of 26 mm. The largest peak-to-peak amplitude of skin displacement was for marker Rad-3 in the direction of the z-axis, which showed a range of motion of 17.8% of segment length or approximately 65 mm. The smallest peak-to-peak amplitude of skin displacement was for marker Rad-6 in the direction of the y-axis, which showed a range of motion of 0.8% of segment length or approximately 3 mm. The maximal s.d. for each marker between subjects was 1.4–5.4% of the segment length, with

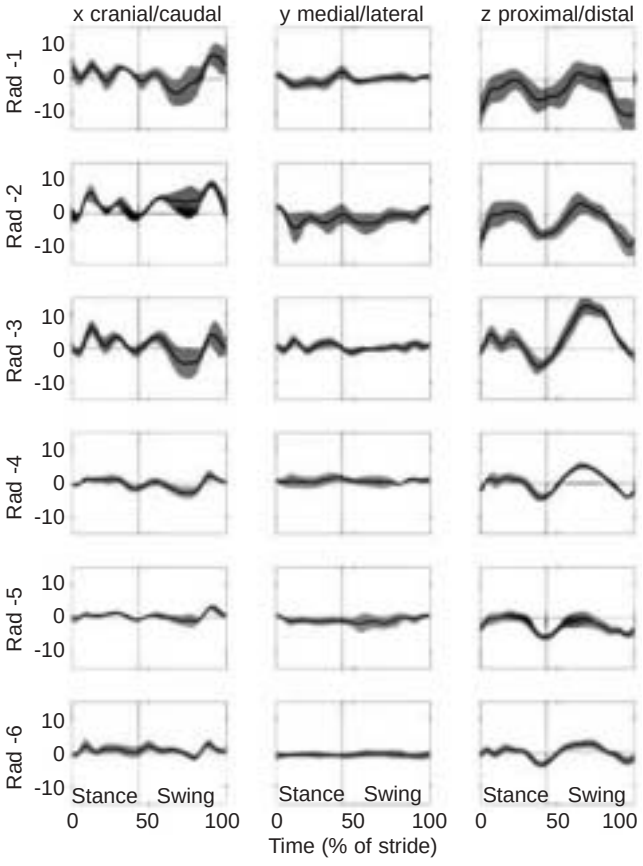

Fig 2: Standard deviations of real skin displacement (shaded area) and skin displacement calculated from the model (black line) for each 3D coordinate of each marker (from Rad-1–Rad-6) on the radial segment plotted as % of segment length. Data for n = 4 except n = 3 for Rad-3. Coordinates x, y and z represent the cranial/caudal, medial/lateral and proximal/distal directions, respectively. Values are described from 0% as the standing pose. Vertical line indicates the transition from stance phase to swing phase.

the average being 3% of segment length. This corresponds to an approximate displacement of 11 mm.

The skin displacement patterns for all markers in the same directions x and z showed similar patterns with higher amplitudes at the proximal locations. The displacement in direction y showed smaller movements compared with that in the x and z directions. Mean ± s.d. peak skin displacements averaged over the 3 markers on the proximal radius and expressed as a percentage of radial length in the x, y and z directions were 10.7 ± 0.5, 4.6 ± 1.5 and 14.5 ± 2.9%, respectively. For the 3 markers on the distal radius, the equivalent displacements were 4.7 ± 0.6, 1.7 ± 0.8 and 7.3 ± 1.8%.

The average number of harmonics required to model the skin displacements were 8, 3 and 10 for the x, y and z directions, respectively. The model showed a good fit to the actual skin data, with most values for the RMS fit error being well below the peak-to-peak amplitude of the displacement itself (Table 3). The largest RMS fit error for the markers was the y-axis of Rad-1, Rad-4 and Rad-5 at 0.41% of segment length.

Discussion

In the lower parts of limbs, for example at sites adjacent to fetlock joints, 2D skin displacements can be modelled as a simple linear regression model of the joint angle (van Weeren *et al.* 1988), but this method is impractical for modelling the complicated pattern of skin displacement in the upper parts of limbs. The best and most intuitive way to establish a model for a periodic data set is to use a Fourier series. The periodic nature of skin displacement at trot lends itself to being modelled with a truncated Fourier series (Cappozzo *et al.* 1975). The general displacement patterns were reproducible between subjects and this was reflected in the low fit errors. Substantial y-axis skin displacement artefacts were recorded in the study, which points to the fact that the 3D nature of the artefacts must be taken into account.

One of the practical considerations in placing skin markers is the need to avoid merging of skin-based markers with bone-based triads during data collection. The relatively large size of the radial segment allows adequate space for placement of 6 skin-based markers. On smaller segments, however, it is more difficult to place sufficient skin markers in locations that do not merge with the bone markers. The radial segment offers a suitable site for percutaneous insertion of a bone pin. Such sites should have the bone located subcutaneously without intervention of locomotor tissues, such as muscle, tendon or ligament, between skin and bone. A minimum of 3 markers must be attached to the bone pin to track bone movements adequately.

Larger skin displacements found at the proximal locations were consistent with the results of the 2D study of van Weeren *et al.* (1990b). Usually, the largest displacements are in the z-axis, i.e. along the axis of segment. Maximal skin displacement in z-axis at the proximal end of the segment could be up to 18% of segment length. Therefore, skin displacement in equine gait analysis may account for major errors in applied biomechanical research and should be corrected (van Weeren *et al.* 1992).

Data from this 3D study can be compared with the earlier 2D data (van Weeren *et al.* 1990b) for x-forward/backward and z-proximal/distal directions only for the sites Rad-1 (proximal radius) and Rad-6 (distal radius) when the relevant data in the present study are converted into absolute values. Taking the average length of the radius as 369 mm, the skin displacements were similar for Rad-6 (in x direction: 15 ± 7 mm in this study, 13 ± 8 mm in the former study; in z direction: 23 ± 5 mm in the present study, 29 ± 3 mm in the former study), and also for the z direction at site Rad-1 (48 ± 19 mm in the present study 45 ± 10 mm in the former study), but not for the x direction at that site (41 ± 20 mm in the present study and less than the detection level which was 11 mm in the former study). In general there was a very good, albeit not perfect agreement. One reason for different values is that the x and z directions of the BCS used in this study are a little different from the x and z directions of the GCS which was used in the 2D studies. In addition to this, a misalignment of the BCS could cause some differences to skin displacements in all 3 directions; and subjects of different sizes have different skin displacements.

In Table 3, the fact that the s.d. is higher than the peak amplitude in y direction for the distal markers indicates that the pattern varies between horses. However, the fact that these displacements are so small indicates that correction in this direction may not be necessary or desirable.

Skin displacements in the y direction at the sites on the distal radius are so small that they might be considered negligible. However, those over the proximal parts of the radius could be up to 6.4% of the length of radial segment, which is about 23 mm in absolute values. This value is large compared with the skin displacements in the x direction at sites over the distal part of the radius. Therefore, the skin displacements over the radius in the

TABLE 2: Truncated Fourier series coefficients (p and q) for determining the 3D skin displacement corrections for 6 radius skin markers (Rad-1–6) at trot

	Rad-1			Rad-2			Rad-3		
	x	y	z	x	y	z	x	y	z
p0	1.0554	-0.16436	-3.4664	3.1844	-1.4349	-2.1403	0.72363	0.41212	3.1758
p1	1.9302	-0.23249	-1.628	1.2535	0.73971	-0.71075	0.44388	0.43146	0.67971
p2	1.5763	0.41511	-3.2546	-0.18726	0.46852	-3.0681	1.4299	-0.26609	-3.3238
p3	-0.16789	0.19353	-0.56306	-0.47554	0.35204	-0.4141	-0.64126	0.36584	-0.3855
p4	-0.68458	0.16558	-0.05277	-1.1714	0.93049	-0.38484	-0.9187	-0.5172	0.27063
p5	-0.69172		0.25351	-1.3905	0.77383	-0.28791	-1.216	-0.28595	-0.09614
p6	-0.14684		-0.15062	-0.49651		-0.22279	-0.43643		-0.16818
p7	0.22948		-0.23994	-0.14307		-0.20107	0.19409		-0.39471
p8	0.24788		-0.22077	-0.07997		-0.31484	0.25356		-0.46241
p9	0.14658		-0.16881	0.07654		-0.15087			-0.19975
p10	0.11103		-0.1237	0.08235		-0.08498			-0.11433
q1	1.2906	-0.53881	-0.74022	-1.5227	-0.46783	-0.68346	2.2091	0.38438	-5.618
q2	-1.6195	-0.71752	2.8978	0.17463	-1.0164	3.1302	0.68443	-0.37331	3.1205
q3	-1.2801	0.47142	0.51986	-1.4363	0.25525	0.07918	-1.8303	0.10574	0.09099
q4	0.17395	-0.4290	0.65712	0.09859	-0.47698	0.77006	0.17479	0.18051	0.54065
q5	-1.4328		0.88158	-0.96525	0.28753	0.67921	-0.83906	-0.36699	0.8881
q6	-0.40168		-0.09456	-0.63373		0.09112	-0.73173		0.35913
q7	-0.16027		0.11375	-0.2826		0.21232	-0.1148		0.03482
q8	0.09273		0.02327	-0.16114		0.2011	0.07057		0.14673
q9	-0.07819		0.02992	-0.16029		0.07948			0.00413
q10	-0.07222		0.10312	-0.17216		0.08822			0.03211
	Rad-4			Rad-5			Rad-6		
	x	y	z	x	y	z	x	y	z
p0	0.21	-0.62787	0.36428	0.4999	-0.74356	-2.0792	0.68348	-0.66773	0.06135
p1	0.84081	-0.17855	-0.36324	0.48937	0.61678	0.43431	-0.03054	-0.08876	-0.13658
p2	0.54231		-1.9175	0.32301		-1.3403	0.41788		-1.1352
p3	-0.32929		-0.13855	-0.02226		0.00352	-0.16664		-0.20469
p4	-0.29819		0.12319	-0.13827		0.1114	-0.20251		0.3557
p5	-0.57426		-0.1708	-0.53794		-0.29123	-0.79205		-0.13336
p6			0.00049			-0.05918	-0.19548		0.10188
p7			-0.00114				-0.20101		0.15331
p8			-0.08725				0.10188		0.01388
p9			-0.09348				0.03554		-0.01459
p10			-0.07096				0.07989		-0.03037
q1	1.047	0.22196	-1.7795	0.40064	-0.04195	0.4393	0.31202	-0.11389	-1.0745
q2	0.0523		2.7544	-0.20866		2.2193	0.06652		1.7798
q3	-1.1950		-0.1155	-0.90411		-0.33517	-0.52392		-0.26938
q4	0.0428		0.6536	-0.08829		0.50994	-0.15396		0.39956
q5	0.0891		0.42274	-0.22375		0.16132	0.24139		0.12843
q6			0.26731			0.19516	0.22462		0.18603
q7			0.26369				0.05254		0.30861
q8			0.26962				-0.14356		0.26882
q9			0.10183				-0.22574		0.12527
q10			0.08084				-0.16987		0.09771

TABLE 3: Descriptive statistics of the modelled skin displacement for each skin surface marker in 3 dimensions. The order indicates the optimal number of harmonics in the truncated Fourier series model. The mean offset from the standing pose location (p0), the difference between the actual displacement and the model (RMS) and the peak-to-peak amplitude of the skin displacement calculated using the model (Peak amp) along with the maximal standard deviation between subjects (Max s.d.) are indicated as percentages of the radius segment length

	x (cranial/caudal)					y (medial/lateral)					z (proximal/distal)				
Marker	Order	p0	RMS	Peak amp	Max s.d.	Order	p0	RMS	Peak amp	Max s.d.	Order	p0	RMS	Peak amp	Max s.d.
Rad-1	10	1.06	0.19	11.2	5.4	4	-0.16	0.41	4.0	2.2	10	-3.47	0.24	13.1	5.1
Rad-2	10	3.18	0.25	10.3	4.7	5	-1.44	0.24	6.4	4.5	10	-2.14	0.25	12.6	3.9
Rad-3	8	0.72	0.17	10.5	4.8	5	0.41	0.36	3.5	1.9	10	3.17	0.20	17.8	3.3
Rad-4	5	-0.21	0.22	5.2	1.7	1	0.63	0.41	1.9	2.2	10	0.36	0.18	9.4	2.3
Rad-5	5	0.50	0.28	4.0	2.0	1	-0.74	0.41	2.5	2.8	6	-2.08	0.27	6.2	2.3
Rad-6	10	0.68	0.20	4.2	1.9	1	-0.68	0.20	0.8	1.4	10	0.06	0.17	6.2	1.5

y direction must be taken into account when using surface markers located in the proximal part of the radius to calculate the 3D kinematics of joints, because a small skin displacement could lead to a large difference in joint angle change (van Weeren *et al.* 1990c). The effects of skin displacements on the 3D kinematics of joints will be addressed in the future.

In practice, the positions of skin-based markers can be corrected by:

$$\hat{p}_s(t) = p_s(t) + \hat{D}_n(t)L$$

where L is the length of the segment. When studies involve

invasive procedures, the onus is on the researcher to minimise the number of subjects. The horses used in this study were similar in size and type, which tends to reduce variability between subjects. Although greater subject numbers are typically perceived as beneficial, the number of horses used in invasive studies needs to be restricted. The expression of skin displacement as a percentage of segment length allows for the use of correction models in horses of a different size to those used in the test group, but application of the models to horses of different sizes and conformation may give rise to errors in predicting skin displacements, because both size and conformation of horses determine the pattern of skin displacement (van Weeren *et al.* 1992).

In this study, the 3D skin displacement patterns for redundant marker sets on the radius of the right forelimb of horses at trot have been quantified. The displacement patterns were successfully modelled as truncated Fourier series, which has previously been used successfully for 2D analysis. The results were expressed in local bone coordinates and scaled to segment length. The data from this investigation may be used to develop a correction procedure to reduce the effect of skin motion artefacts on 3D kinematics of the radius and joints relative to the radius segment. Further development will improve the precision of bone movement reconstruction by tracking surface markers, thereby providing a more sensitive measure for kinematic analysis.

Acknowledgement

We would like to acknowledge the McPhail endowment for financial support of this work.

Manufacturers' addresses

[1]Motion Analysis Corporation, Santa Rosa, California, USA.
[2]AMTI, Watertown, Massachusetts, USA.

References

Arun, K., Huang, T. and Blostein, S. (1987) Least-squares fitting of two 3-d point sets. *IEEE Trans. Patt. Anal. Machine Intell.* **9**, 698-700.

Cappozzo, A., Leo, T. and Pedotti, A. (1975) A general computing method for the analysis of human locomotion. *J. Biomech.* **8**, 307-320.

Cappozzo, A., Cappello, A., Della Croce, U. and Pensalfini, F. (1997) Surface-marker cluster design criteria for 3-D bone movement reconstruction. *IEEE Trans. Biomed. Eng.* **44**, 1165-1174.

Hanson, R. and Norris, M. (1981) Analysis of measurements based on the singular value decomposition. *SIAM J. Sci. Stat. Comput.* **2**, 363-373.

Lanovaz, J.L., Khumsap, S., Clayton, H.M., Stick, J.A. and Brown, J. (2002) Three-dimensional kinematics of the tarsal joint at the trot. *Equine vet J., Suppl.* **34**, 308-313.

Reinschmidt, C., van den Bogert, A.J., Nigg, B.M., Lundberg, A. and Murphy, N. (1997a) Effect of skin movement on the analysis of skeletal knee joint motion during running. *J. Biomech.* **30**, 729-732.

Reinschmidt, C., van den Bogert, A.J., Murphy, N., Lundberg, A. and Nigg, B.M. (1997b) Tibiocalcaneal motion during running - measured with external and bone markers. *Clin. Biomech.* **12**, 8-16.

Soderkvist, I. and Wedin, P.A. (1993) Determining the movements of the skeleton using well-configured markers. *J. Biomech.* **26**, 1473-1477.

van den Bogert, A.J., van Weeren, P.R. and Schamhardt, H.C. (1990) Correction for skin displacement errors in movement analysis of the horse. *J. Biomech.* **23**, 97-101.

van Weeren, P.R. and Barneveld, A. (1986) A technique to quantify skin displacement in the walking horse. *J. Biomech.* **19**, 879-883.

van Weeren, P.R., van den Bogert, A.J. and Barneveld, A. (1988) Quantification of skin displacement near the carpal, tarsal and fetlock joints of the walking horse. *Equine vet. J.* **20**, 203-208.

van Weeren, P.R., van den Bogert, A.J. and Barneveld, A. (1990a) Quantification of skin displacement in the proximal parts of the limbs of the walking horse. *Equine vet. J., Suppl.* **9**, 110-119.

van Weeren, P.R., van den Bogert, A.J. and Barneveld, A. (1990b) A quantitative analysis of skin displacement in the trotting horse. *Equine vet. J., Suppl.* **9**. 101-109.

van Weeren, P.R., van den Bogert, A.J., Barneveld, A., Hartman, W. and Kersjes, A.W. (1990c) The role of the reciprocal apparatus in the hind limb of the horse investigated by a modified CODA-3 opto-electronic kinematic analysis system. *Equine vet. J., Suppl.* **9**. 95-100.

van Weeren, P.R., van den Bogert, A.J. and Barneveld, A. (1992) Correction models for skin displacement in equine kinematic gait analysis. *J. equine vet. Sci.* **12**, 178-192.

Woltring, H.J. (1986) A FORTRAN package for generalised cross-validatory spline smoothing and differentiation. *Adv. Eng. Softw. Workst.* **8**, 104-113.

Woltring, H.J. (1990) Model and measurement error influences in data processing. In: *Biomechanics of Human Movement: Applications in Rehabilitation, Sports and Ergonomics*, Eds: N. Berme and C. Capozzo, Bertec Corporation, Worthington, Ohio. pp 203-237.